European Journal of Pharmaceutical Sciences 218 (2026) 107429

Contents lists available at ScienceDirect

European Journal of Pharmaceutical Sciences

journal homepage: www.elsevier.com/locate/ejps

Development and *in vitro/in vivo* evaluation of polymeric dissolving microneedle formulation for psoriasis treatment

Meryem Kaplan [a,b,1], Fatma Betül Arslan [a,1], Süleyman Can Öztürk [c], Sıla Ulutürk [d], Çisel Aydın Meriçöz [e], Güneş Esendağlı [d], Sema Çalış [a], Kivilcim Ozturk [a,*]

[a] Department of Pharmaceutical Technology, Faculty of Pharmacy, Hacettepe University, 06100, Ankara, Turkiye
[b] Department of Pharmaceutical Technology, Faculty of Pharmacy, Süleyman Demirel University, 32260, Isparta, Turkiye
[c] Centre for Laboratory Animals Research and Application, Hacettepe University, Ankara, Turkiye
[d] Department of Basic Oncology, Hacettepe University Cancer Institute, 06100, Ankara, Turkiye
[e] Department of Pathology, Faculty of Medicine, Koc University, 34450, Istanbul, Turkiye

ARTICLE INFO

Keywords:
Psoriasis
Microneedle
Stattic
Secukinumab
Immunotherapy
Transdermal drug delivery

ABSTRACT

Psoriasis is an inflammatory autoimmune skin disease that significantly impacts quality of life. The chronic and recurrent nature of the disease can last a lifetime. Current conventional treatment options have several drawbacks, including inadequate or short-lived efficacy, issues with tolerability and adherence, practical limitations associated with topical applications and phototherapy, and significant safety and cost concerns related to systemic treatments. Generally, symptomatic treatments are applied, but complete recovery is rarely achieved. Researchers are exploring alternative treatment approaches, such as biologically based therapies. These therapies specifically target the immune mechanisms involved in psoriasis and offer advantages such as more reliable disease control, noticeable improvements in patients' quality of life, and a more favorable safety profile compared to conventional treatments. One innovative approach being investigated for the treatment of psoriasis is the use of microneedles as a transdermal drug delivery strategy, which has shown promising results in research. In this study, a biocompatible polymeric dissolving microneedle formulation composed of hyaluronic acid and sucrose was prepared using micro-molding. Microneedles were loaded with secukinumab (a human monoclonal antibody specific to IL-17A) and Stattic (a STAT3 inhibitor) for a combined treatment approach. It was expected that applying the microneedles directly to the psoriasis plaques would increase the localized drug concentration. Following *in vitro* characterization and cell culture studies, a psoriasis model was established in adult mice. The therapeutic effects of the microneedles containing secukinumab and Stattic (both individually and simultaneously loaded) were compared to control groups. Lesion progression was visually monitored and histologically examined following treatment. The results indicated that the secukinumab-loaded microneedles provided a more effective treatment at lower doses.

1. Introduction

Psoriasis is a chronic inflammatory autoimmune disease of the skin, characterized by abnormal epidermal differentiation and hyperproliferation (Bodemer, 2023; Pradhan et al., 2018). It typically manifests in young people in their 20s (Reichrath and Holick, 2018) and affects approximately 2% of the population in Western countries (Miao et al., 2025; Sun et al., 2024). The most common form of the disease is plaque psoriasis, which accounts for about 90% of cases and causes the skin to develop scaly, red lesions. Plaques may range from a few scattered lesions to covering the entire body (Das et al., 2024; Worm and Sterry, 2006). The development of psoriasis is influenced by genetic factors and aging. Additionally, environmental factors such as physical trauma, infections, hypocalcemia, stress, and certain medications play a significant role in triggering psoriatic flares (Bodemer, 2023; Miao et al., 2025).

Current treatment strategies for psoriasis aim to manage symptoms, improve the quality of life, and prevent disease progression (Lee and

* Corresponding author.
E-mail address: k.ozturk@hacettepe.edu.tr (K. Ozturk).
[1] Meryem Kaplan and Fatma Betül Arslan contributed equally to this article.

https://doi.org/10.1016/j.ejps.2026.107429
Received 17 September 2025; Received in revised form 15 December 2025; Accepted 5 January 2026
Available online 6 January 2026
0928-0987/© 2026 The Authors. Published by Elsevier B.V. This is an open access article under the CC BY-NC license (http://creativecommons.org/licenses/by-nc/4.0/).

Kim, 2023). A variety of therapeutic options are available to achieve these goals. Topical agents such as corticosteroids, vitamin D analogues, and dithranol are commonly used for symptomatic relief in mild cases (Ramic and Sator, 2023). For moderate to severe psoriasis, phototherapy (including natural sunlight, psoralen ultraviolet A, broadband or narrowband ultraviolet B, and pulsed dye laser) and systemic conventional drugs (such as methotrexate, cyclosporine, apremilast, and systemic retinoids) can help alleviate symptoms and induce temporary remission(Ighani et al., 2019; Zhang and Wu, 2018). Biologic agents (such as infliximab, adalimumab, and secukinumab) specifically target immune pathways and provide sustained suppression of pathogenic immune activity. This helps slow or prevent disease progression in severe or refractory cases (Lé and Torres, 2022; Raharja et al., 2021). Although psoriasis symptoms can be managed with available treatment options, the efficacy and safety profiles of conventional treatments may vary (Dubey et al., 2017; Papp and Lebwohl, 2018).

Recent advancements in understanding the pathophysiology of psoriasis have led to the emergence of biologic therapies and immunotherapeutics that selectively target the immune mechanisms underlying the disease. The first biologic agents approved for moderate-to-severe psoriasis were TNF-α inhibitors, including adalimumab, etanercept, infliximab, and certolizumab. Newer therapies include interleukin-17 (IL-17) inhibitors (e.g., ixekizumab and secukinumab), interleukin-12/interleukin-23 (IL-12/IL-23) inhibitors (e.g., ustekinumab), and IL-23 inhibitors (e.g., risankizumab and guselkumab). These agents play an important role in the treatment of psoriasis by targeting specific cytokines involved in the inflammatory pathways (Alexander and Nestle, 2017; Hawkes et al., 2018; Raharja et al., 2021). Other treatment approaches involve using multiple agents in combination to enhance efficacy and minimize off-target effects, utilizing biomarkers for treatment selection and monitoring, and exploring gene- and cell-based therapies (Lee and Kim, 2023).

This study focuses on two active substances: Secukinumab (Sec), a recombinant human monoclonal IgG1 antibody that specifically binds to IL-17A, which the FDA has approved for treating moderate to severe plaque psoriasis and active psoriatic arthritis in adults; and Signal Transducer and Activator of Transcription-3 (STAT3), a cytoplasmic transcription factor encoded by the STAT3 gene (Berg et al., 2021; Fletcher et al., 2008; Yang et al., 2016). IL-17 is a pro-inflammatory cytokine that plays a significant role in the chronic inflammation process associated with various diseases, including allergies and autoimmune diseases like psoriasis. The activation of IL-17A in psoriasis leads to excessive proliferation of keratinocytes and chronic skin inflammation. Using Secukinumab in the treatment of psoriasis is a rational approach, as it helps regulate wound-healing processes and prevents the production of pro-inflammatory cytokines by blocking IL-17 from binding to its receptor (Huangfu et al., 2023; McGeachy et al., 2019). Studies indicate that STAT3 stimulates the IL-17A gene in T cells, which is crucial for psoriasis treatment (Gharibi et al., 2020) and plays a critical role in the transcriptional regulatory network underlying the disease's pathogenesis (Ti et al., 2024). Furthermore, STAT3 activation suppresses the differentiation of regulatory T cells (Tregs), essential for preventing the onset and progression of autoimmune diseases (Fletcher et al., 2008; Gharibi et al., 2020). Given the role of STAT3 in immune response regulation and autoimmunity, inhibiting STAT3 is considered significant in alleviating or treating autoimmune diseases (Gharibi et al., 2020). Therefore, the combination of Stattic (St), a STAT3 inhibitor, with Sec is expected to enhance treatment efficacy. Utilizing this combination in a microneedle delivery system aims to improve efficiency at lower doses, potentially surpassing existing formulations in efficacy. This approach not only presents a novel combination strategy but also enables the development of a novel formulation.

In recent decades, numerous studies have focused on strategies to enhance the efficiency of topical drug delivery to psoriatic plaques. Among these strategies, hydrogels, nanoparticles, microneedles (MNs), and nanofibers have been explored. Notably, nanoparticles have been the most extensively studied delivery system, while microneedles and nanofibers are emerging as promising alternatives (Lee and Kim, 2023). Additionally, several studies (Du et al., 2024; Huang et al., 2025; Jha et al., 2024; Li et al., 2024; Xia et al., 2024; Zeng et al., 2025) have investigated the incorporation of drug-loaded nanoparticles into MNs. The transdermal delivery of therapeutic compounds using microneedles (MNs) is a rapidly developing approach, despite its drawbacks. For example, the loading capacity and dermal absorption of the active substance are limited by the surface area of the patch. Microneedles can also cause temporary inflammation and allergic reactions. Factors such as skin hydration and individual variations in the thickness of the stratum corneum and other skin layers can significantly influence drug delivery. Additionally, the tips of solid MNs can break off and remain embedded in the skin upon patch removal (Guillot et al., 2020; Jung and Jin, 2021; Nagarkar et al., 2020). Despite these limitations, microneedles have several advantages that make them a suitable delivery system. They facilitate self-administration and have a single-use design, minimizing the need for healthcare personnel and reducing the risk of cross-contamination. Microneedles can deliver both small molecules and complex therapeutic agents. Moreover, they may provide long shelf life and stability at room temperature, making storage and distribution easier. Patches can be easily removed in the event of an adverse reaction and enable targeted delivery to specific skin sites or skin-resident cells, alongside controlled drug release (Ghaferi et al., 2024; Kochhar et al., 2019; Sartawi et al., 2022; Zhao et al., 2020).

In this study, dissolving microneedles based on hyaluronic acid (Sodium hyaluronate) and sucrose were formulated as the preferred drug delivery system. Hyaluronic acid (HA) served as the primary polymer in the matrix. HA is a water-soluble polymer with a viscoelastic structure that is naturally present in various tissues, including the skin, synovial fluid, skeletal tissue, lungs, kidneys, brain, aorta, and vitreous fluid (Kang et al., 2022; Salih et al., 2024; Valachová and Šoltés, 2021). The FDA approved HA for injection-based soft tissue augmentation in 2003 Since then, numerous products have been developed, leading to its widespread use in cosmetics (de Sousa et al., 2023). The properties of HA, such as high biocompatibility, the ability to facilitate microneedle fabrication without requiring heating, and relatively low cost, make it a suitable candidate for microneedle matrices. However, pre-formulation studies have shown that microneedles made solely of HA are prone to bending or breaking during extraction. To address this issue, sucrose was incorporated as an additional polymer, as several studies have reported that it enhances the flexibility of microneedle patches(Du and Sun, 2020; He et al., 2019). We developed HA and sucrose based polymeric dissolving microneedles co-loaded with the STAT3 inhibitor Stattic and IL-17A inhibitor secukinumab using the micro-molding technique. Both *in vitro* and *in vivo* characterization studies were conducted. The goal of our research was to propose an alternative treatment strategy that could reduce the necessary drug dosage for therapy, improve therapeutic efficiency, and enhance patient compliance.

2. Materials and methods

2.1. Materials

Secukinumab was purchased from Biolegend (CA, USA). Stattic was obtained from MedChemExpress (NJ, USA). Sodium hyaluronate (Mw <5000 Da) was purchased from Kangcare Bioindustry (Nanjing, China). Sucrose was obtained from Merck (Darmstadt Germany). Microneedle templates (mold) were supplied by Smicna Pte. Ltd. (Pioneer Junction, Singapore). Imiquimod was obtained from Cayman Chemical (MI, USA). BCA Protein Assay Kit was obtained from Takara Bio Inc. (Shiga, Japan). L929 cells were purchased from the ATCC (MD, USA). Dulbecco's modified eagle medium (DMEM), fetal bovine serum (FBS), penicillin, and streptomycin (10000 U/mL and 10 mg/mL, respectively) solutions were obtained from Biological Industries (Connecticut, USA). Ficoll, methylthiazolyltetrazolium (MTT), and methylene blue were purchased

Table 1
Codes and descriptions of the formulations used in experiments.

Formulation Code	Description
Sec	Secukinumab
St	Stattic
Blank MN	Blank (drug-free) microneedles
Sec-loaded MN	Secukinumab loaded microneedles
St-loaded MN	Stattic loaded microneedles
Sec/St-loaded MN	Secukinumab and Stattic loaded microneedles
Sec-loaded MNMS	Matrix solution* for secukinumab loaded microneedles
St-loaded MNMS	Matrix solution* for Stattic loaded microneedles
Sec/St-loaded MNMS	Matrix solution* for secukinumab and Stattic loaded microneedles

* Matrix solution= sucrose + sodium hyaluronate + DMEM

from Sigma-Aldrich Co. (St. Louis, MO, USA). Sodium dodecyl sulfate and dimethylformamide were purchased from J.T. Baker (Deventer, The Netherlands). All Type I water was of analytical grade (Milli-Q Plus System–Millipore/Millipore Corporation, Burlington, MA, USA).

2.2. Quantification of stattic and secukinumab

The quantification of Stattic was performed using the HPLC method (Agilent 1200 Infinity-DAD detector), as described in our previous study (Arslan et al., 2023). In summary, the analysis was conducted at a temperature of 25 ± 1°C using a C18 column (250 × 4.0 mm; 5 µm). The mobile phase consisted of acetonitrile (60%) and ultra-pure water (40%) at a flow rate of 1.0 mL/min, and results were monitored at 215 nm.

The amount of Sec in MNs was quantified using the BCA assay. Following the manufacturer's protocol, standard solutions of BSA ranging from 5 to 200 ppm were prepared by diluting the stock solution of bovine serum albumin (2 mg/mL) with a pH 7.4 PBS buffer. These solutions were then incubated with a mixture of Reagent A and Reagent B (100:1) in a 96-well plate for 1 hour in the dark at 37°C. The absorbance of samples was measured at 562 nm.

2.3. Preparation of dissolving MNs

The dissolving microneedles were prepared using a cost-effective micro-molding technique. Sodium hyaluronate (43.5% w/w) and sucrose (13% w/w) were dissolved in 1.5 mL of deionized water to obtain the polymer matrix. To ensure effective solubilization and eliminate air bubbles, the polymer matrix components were centrifuged three times at 2800 g for 3 minutes. Microneedle molds were obtained with a height of 400 µm, a base width of 150 µm x 150 µm, and a peak-to-peak distance of 500 µm. After placing the matrix solution into the silicone molds, centrifugation was performed four times at 6200 g for 5 minutes to ensure complete filling of the microneedle mold cavities. After each centrifugation cycle, the polymer solution was added onto the mold (Lee et al., 2008). To prepare drug-containing microneedles (Table 1), two additional steps were performed before casting the polymer matrix solution into the molds: St (0.5 mg per MN patch) was dispersed; Sec (65 µg per MN patch) was dissolved in the polymer matrix solution. Finally, the MNs were dried at room temperature in a desiccator for 36 hours (Fig. 1).

2.4. In vitro characterization of MNs

2.4.1. Morphology

The morphology of the MNs was evaluated using a polarized light microscope (Leica DM500, Wetzlar, Germany). To enable visualization under the microscope, MNs were loaded with a fluorescent dye, indocyanine green. Images were captured with a light microscope equipped with fluorescence imaging. Fluorescent dye-loaded MNs were fabricated as follows: 3 mg of indocyanine green dye was added to the previously prepared polymeric matrix, and the matrix was centrifuged three times at 2800 g for 3 min. After centrifugation, MNs were prepared as previously described.

Additionally, the morphology of blank MNs was analyzed using scanning electron microscopy (SEM) at the Middle East Technical University (METU) Central Laboratory, Turkey, following the methodology described by Coulman et al. (Coulman et al., 2009). As sputter coating was not required, the samples were directly mounted on a metal plate and examined using a QUANTA 400F Field Emission Scanning Electron Microscope. This analysis provided detailed insights into the surface characteristics of both the needle and patch components.

2.4.2. Mechanical performance of blank polymeric MN arrays

The mechanical properties of blank MNs were assessed (n=3) with a TA.XT plus texture analyzer (Stable Micro Systems, Surrey, UK) (Yan et al., 2021). The MN patch was positioned on a flat, rigid aluminum plate with the tips facing upwards. A flat-head stainless steel cylindrical probe (p/05) was used to apply an axial force to the tips of the MNs at a constant speed of 1 mm/s, with a trigger force set at 0.049 N. The force at which the tips of the MNs began to deform (microneedle resistance) was recorded. The deformation of microneedle arrays was also verified through light microscopy.

2.4.3. In vitro dissolution study

In vitro dissolution studies were conducted using a setup with an artificial membrane, in which Parafilm® was used as the membrane for microneedle arrays (a modified version of the method developed by Larrañeta et al. (Larrañeta et al., 2016)). Sink conditions were readily

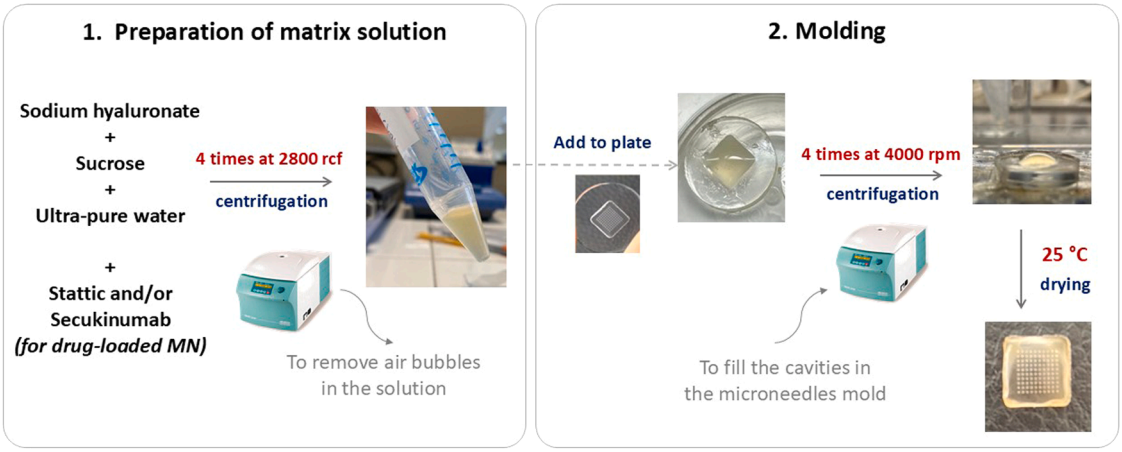


Fig. 1. Fabrication of MNs by molding technique.

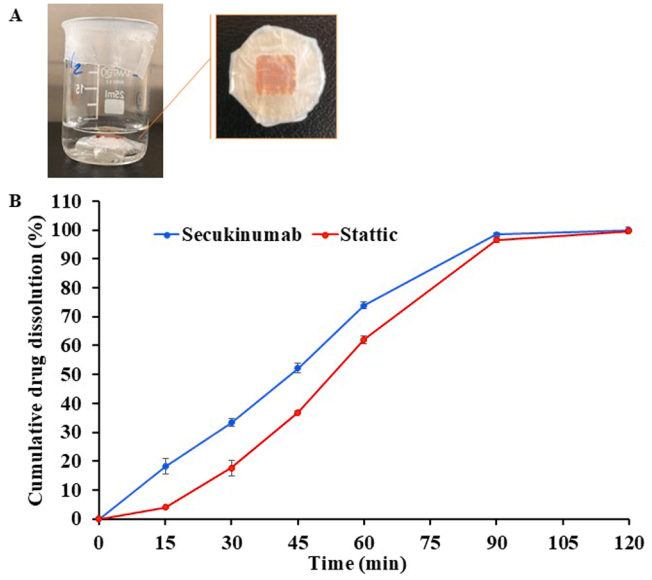


Fig. 2. A. Representative image of the experimental setup for drug release from microneedles; B. *In vitro* dissolution profile of Sec and St from dissolving MNs (pH 5.6) (n=3).

maintained for secukinumab; however, strict sink conditions could not be fully ensured for Stattic due to its limited aqueous solubility. Initially, strips of Parafilm® measuring 3.5 × 3 cm were cut and then stretched to twice their original length using the tensile gripper of the XT-Plus Texture Analyzer. This process resulted in a thinner membrane that allowed the microneedles to penetrate the Parafilm® without breaking. After placing the pre-stretched films on the needles, the p-05 probe of the same device was used to apply pressure to the microneedle at a speed of 0.5 mm/s until a force of 40 N, which was required for the needles to penetrate the Parafilm® layer, was achieved. This setup ensured that the microneedles would come into contact with the dissolution medium while the patch part remained isolated. A metal weight was placed on the back (patch) of the MNs to prevent the MNs from floating freely in the dissolution medium. Additionally, the Parafilm® layer surrounding the assembly was thermally sealed to create a hermetic pouch (Rehman et al., 2021). The prepared setup was placed in a 25 mL beaker, into which 5 mL of dissolution medium (pH 5.6 phosphate buffer) was added. The beaker was then sealed with Parafilm® (Fig. 2A). The experiment was conducted in a water bath equipped with a horizontal shaker, operating at a shaking speed of 140 strokes per minute and 32°C (skin surface temperature). Microneedle arrays (n=3) placed in the water bath were sampled at various time intervals: 15, 30, 45, 60, 90, and 120 minutes. A previously validated HPLC method was used for the quantification of St, while a BCA kit was used for quantifying Sec.

The KINETDS 3.0 program was used to determine the dissolution kinetics. Cumulative drug dissolution values obtained at predefined time points were manually entered into the program. KINETDS 3.0 subsequently evaluates the dataset against standard kinetic models (e.g., zero-order, first-order, Higuchi, Korsmeyer–Peppas, Weibull) and determines the best fit based on statistical parameters such as the coefficient of determination (R^2) and the model-dependent dissolution constant.

Table 2
Necrosis and inflammation rates under different treatment conditions.

	Mild Necrosis %	Necrosis %	Mild Inflammation %	Inflammation %
No treatment	50	-	-	50
Blank MN	40	-	-	80
Sec-loaded MN	20	4	-	-
St-loaded MN	80	20	20	-
Sec/St-loaded MN	100	-	20	-

2.4.4. *Ex vivo penetration test*

Hairless rat skin (previously sacrificed and kept in the freezer) was used to evaluate the penetration ability of MNs. The skin's temperature was raised to 32°C. It was then stretched and secured to a device using needles. Subsequently, methylene blue-loaded MNs were applied to the skin for 4 minutes. These microneedles were prepared as outlined in Section 2.4.1 (with methylene blue substituting indocyanine green). Fluorescence microscopy was used to visualize the skin before and after the microneedle penetration (Jiang and Lillehoj, 2020).

2.5. *In vitro toxicity study*

The safety studies of MNs were conducted using the L929 fibroblast cell line, and cell viability was evaluated by MTT assay (Cannella et al., 2020). The cells were cultured in DMEM supplemented with 10% FBS and 1% penicillin-streptomycin solution, and were incubated in a humidified atmosphere containing 5% CO_2 at 37°C. The cells were seeded (2×10^4 cells/well) in a 96-well plate and incubated for 24 h. To evaluate the safety of MNs, a blank polymer matrix containing 5 mg of sodium hyaluronate and 1.5 mg of sucrose in DMEM was prepared. This solution was diluted to achieve concentrations ranging from 3.125 to 200 μg/mL, representing different concentrations of sodium hyaluronate, and 50 μL of the matrix solution was applied to each well. Following 24 and 48 hours of incubation, 25 μL of MTT was added to the cells and incubated for 4 hours. After incubation, 80 μL of 23% sodium dodecylsulfate solution (pH 4.7, dissolved in 45% dimethylformamide) was added to the wells, and the plates were kept in the incubator overnight. After 15 hours, optical density was measured spectrophotometrically at 570 nm using an ELISA plate reader, and % viability values (n=4) were calculated.

2.6. *In vivo evaluation of MNs and histopathological assessment*

All experimental procedures and animal handling were conducted in compliance with the ethical approval obtained from the local ethical committee of Kobay Laboratories (Approval number:2020/07-03) and in accordance with relevant guidelines. *In vivo* studies were performed to evaluate the efficacy of MN formulation in C57BL/6J mice. The psoriasis model was developed based on the method described by Sakai et al. (Sakai et al., 2016). To mimic the reference cream (Aldara®, Meda Pharmaceuticals) used in previous studies, vanishing cream was selected as the vehicle, and a 5% imiquimod-containing formulation was prepared as a magistral preparation (Horváth et al., 2019; Sakai et al., 2016). Additionally, a drug-free (blank) cream was formulated as a control to assess the potential effects of the excipients. The cream formulations with (62.5 mg cream containing 3.125 mg imiquimod) or without imiquimod were applied once daily for seven consecutive days to a 3 × 3 cm shaved area on the backs of adult male C57BL/6J mice. Once psoriatic lesions developed, the mice (n=5) were randomly assigned to five groups: Sec-loaded MNs, St-loaded MNs, Sec/St-loaded MNs, blank MNs, and a positive control. MN applications were performed three times at three-day intervals, and the weights of mice were recorded throughout the treatment. The microneedles were left in place for 5 minutes to allow for dissolution. Mice were sacrificed two days after the final application. The formation and progression of psoriatic lesions were visually assessed, and histopathologic examinations were conducted on skin samples collected post-treatment.

For histological evaluation, skin tissues were fixed in 10% neutral buffered formalin, processed routinely, embedded in paraffin, and sectioned to a thickness of 3–4 μm. Hematoxylin–eosin (H&E)–stained slides were examined by a board-certified pathologist blinded to the treatment allocation.

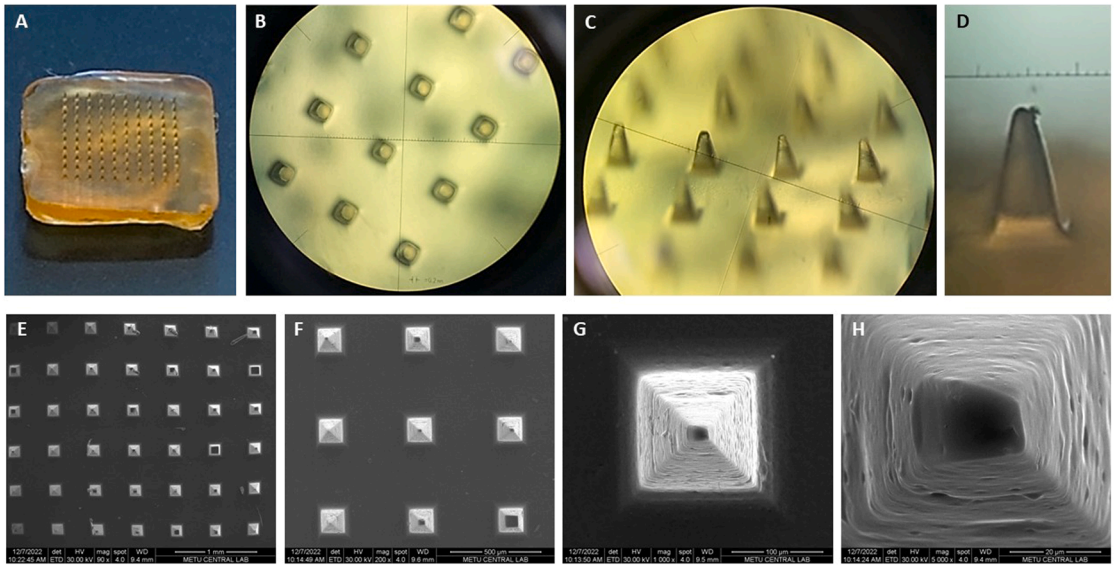


Fig. 3. Representative photograph (A), optical microscopy images (B–D), and SEM images (E–H) of dissolving MNs, with SEM scale ranging from 1 mm to 20 μm.

A semi-quantitative scoring system was applied to assess inflammation and necrosis, based on the approximate percentage of tissue involvement within the dermis and subcutaneous fat: 0%: none; 1–25%: mild; 26–50%: moderate; >50%: severe. This scoring was used independently for both inflammatory infiltrate and necrotic changes. The percentages presented in Table 2 represent these semi-quantitative estimates for each treatment group (derived from blinded slide review).

2.7. Immune function analysis

The potential of St and/or Sec-loaded microneedles to inhibit inflammatory pathways involved in psoriasis immunopathology was evaluated using *ex vivo* splenocyte cultures. For this purpose, freshly prepared microneedle matrix solutions (MNMS) were used. These solutions consisted of sucrose, sodium hyaluronate, DMEM (instead of water), and St and/or Sec. Following the *in vivo* study, spleens were harvested from male C57BL/6 mice and homogenized by adding 3 mL of DMEM onto a 40 μm cell strainer. The resulting spleen cell suspension was subjected to density gradient centrifugation with Ficoll (1.077 g/mL) at 400 g for 25 min at 25°C to isolate splenocytes (Govindarajan et al., 2015).

Splenocytes were seeded into 48-well plates at a density of 3×10^6 cells per well and allowed to adhere for 3 hours under standard incubation conditions. DMEM was used as the control for the drug solutions, while the polymer matrix (sucrose + sodium hyaluronate + DMEM) served as the control for the microneedle groups. Following this, DMEM (drug-solution control), matrix solution (microneedle control), Sec solution, St solution, Sec/St solution, Sec-loaded MNMS, St-loaded MNMS, and Sec/St-loaded MNMS were administered and incubated for an additional 3 hours. After the incubation period, the cells were stimulated with purified anti-mouse CD3 antibodies to induce IL-17 production from T lymphocytes within the splenocyte population (Alunno et al., 2013; Nakae et al., 2003).

The suppressive effects of the treatment and control groups on IL-6, IL-8, and G-CSF cytokine stimulation were assessed using ELISA according to the manufacturer's protocols. Additionally, the extent of STAT3 phosphorylation inhibition was analyzed via Western blotting. ELISA results were obtained by measuring absorbance at 450 nm and 570 nm using a microplate reader.

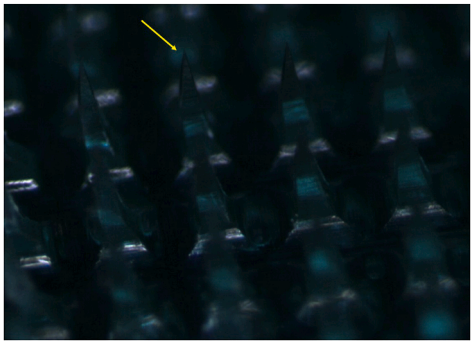


Fig. 4. Microscope images of dissolving MNs loaded with indocyanine green. The yellow arrow marks the microneedle tip.

2.8. Statistical analysis

All values are presented as arithmetic mean ± standard deviation (SD), calculated from at least three independent experiments, unless stated otherwise in the Methods section. Detailed information concerning the statistical methods used can be found in the corresponding figure legends. Statistical analyses were performed with GraphPad Prism software version 9 (GraphPad). Statistical differences between experimental groups were determined using analysis of variance (ANOVA), Student's t-test, or the Mann-Whitney U test, as required. Significance is indicated as follows: $*p < 0.05$; $**p < 0.01$; $***p < 0.001$, $****p < 0.0001$. Comparisons are not statistically significant unless indicated.

3. Results and discussion

3.1. Morphological assessment of microneedles

Dissolving MNs were successfully prepared using the molding technique without causing damage to the needles. It was confirmed by light microscopy and SEM that the microneedle arrays and microneedle tips were produced uniformly, as expected (Fig. 3). The images of the prepared microneedles were consistent with those reported in the literature (Dawud and Abu Ammar, 2023; Gomes et al., 2022; Kim et al., 2020). As part of the fluorescent imaging studies, MNs were loaded with indocyanine green and methylene blue. Indocyanine green was distributed

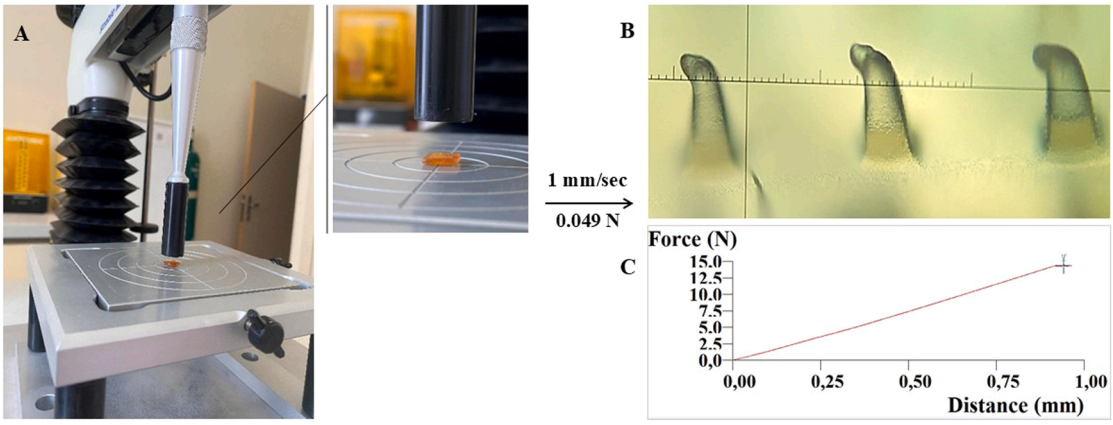


Fig. 5. Texture Analyzer experimental setup used in mechanical resistance studies (A), microscopic examination (10x) of microneedle deformation after force application (B), and force-distance graph (C).

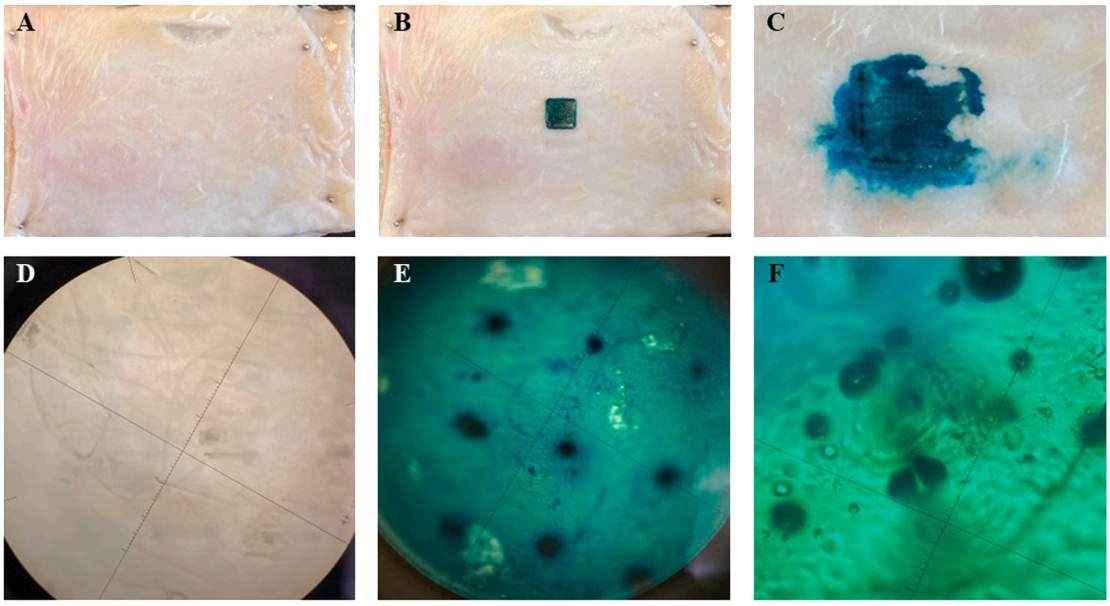


Fig. 6. Macroscopic and microscopic evaluation of methylene blue-loaded dissolving MNs before and after application to healthy rat skin: **A.** Intact and healthy rat skin before MN application (macroscopic view); **B.** Application of methylene blue–loaded dissolving MNs to intact rat skin; **C.** Rat skin immediately after MN penetration, showing dye deposition within the insertion sites; **D.** Microscopic examination of intact and healthy rat skin prior to MN application; **E.** Microscopic examination of rat skin following MN penetration, demonstrating microchannels created by the dissolving MNs; **F.** Microscopic image of the methylene blue–loaded MN array after application, showing loss of needle tips due to dissolution upon skin insertion.

uniformly throughout the entire microneedle, while methylene blue was selectively confined to the needle section (Fig. 4). This strategy aimed to assess the feasibility of loading drugs exclusively in the needle region. Imaging confirmed the successful localization of methylene blue within the needle section, demonstrating the potential of this approach for precise drug delivery.

3.2. *In vitro evaluation of microneedle strength*

A crucial factor in the effectiveness and reliability of microneedles (MNs) is their mechanical strength, which impacts their ability to penetrate the skin during topical application (Chi et al., 2022). HA, the primary component of the microneedle matrix, provides flexibility to the microneedle structure due to its viscoelastic properties (Kang et al., 2022). In a study by Chi et al. (Chi et al., 2022), mechanical strength tests were performed on MNs prepared with HA at molecular weights of 10, 72, and 290 kDa. The results indicated that MNs made with the lowest molecular weight form of HA exhibited the highest mechanical strength. Therefore, in our study, a low molecular weight form of HA (sodium hyaluronate) was selected to enhance mechanical strength. Sucrose was also incorporated into the MN matrix to improve both flexibility during skin insertion and overall durability.

Mechanical strength testing was performed using a Texture Analyzer to measure the force required for microneedle tips to deform (microneedle resistance). Ideally, microneedle arrays should deform under pressure without breaking, ensuring successful skin penetration without structural failure (Alrimawi et al., 2024). The results (Fig. 5) demonstrated that the microneedles withstood a force of 0.049 N applied at approximately 5 mm, exhibiting a resistance of 14.34 N without breaking. Imaging studies using a polarized light microscope confirmed that the microneedle arrays did not break but deformed as expected. These findings indicate that the MN matrix composition (HA and sucrose) has sufficient mechanical strength and flexibility for effective transdermal application.

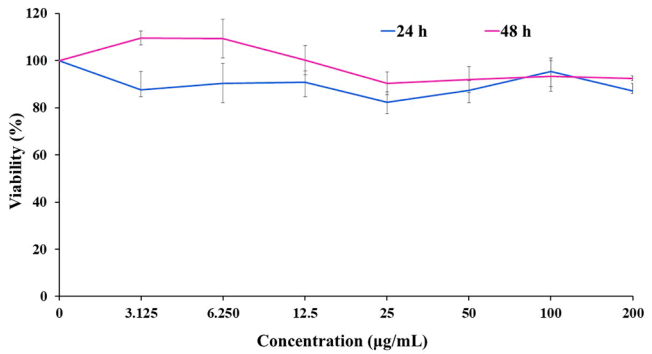


Fig. 7. Cell viability of L929 cells following incubation with MN matrix solution.

3.3. Skin penetration

The penetration capability of microneedles (MNs) into the skin was evaluated through visual inspection and fluorescence microscopy. For this purpose, *ex vivo* penetration studies were conducted with methylene blue-loaded microneedles and rat skin. Pre- and post-penetration images (Fig. 6) indicated that the skin structure was intact before application (Fig. 6A and D), whereas post-application images revealed successful localized penetration at the tip area of the patches (Fig. 6C and E), as expected. Microscopic evaluation results were also consistent with previous findings (Alrimawi et al., 2024; Jang et al., 2020). The tips of the microneedles had completely dissolved within the skin (Fig. 6F). Shin and his team (Shin et al., 2024) developed dissolving microneedles of varying lengths (350, 500, 800 µm) and conducted penetration studies using minipig skin. They concluded that microneedles with a length of 350 µm are capable of effectively penetrating the SC and represent the optimal size for safer and more effective transdermal drug delivery, which supports the chosen microneedle size in our study. In conclusion, a microneedle length of 400 µm was determined to be sufficient for skin penetration, effectively reaching both the outermost SC and the epidermis (Chen et al., 2018), ensuring successful drug delivery to the target site.

3.4. In vitro dissolution rate

The kinetics of drug dissolution in polymeric microneedles depend on the degradation rate of polymers (specifically HA in this study) within the matrix (Lee et al., 2008). For poorly water-soluble drugs, achieving strict sink conditions is often difficult, and further modification of the dissolution medium may interfere with drug release behavior. Accordingly, non-sink conditions have been reported as an alternative for characterizing dissolution profiles in such systems (Phillips et al., 2012). As described in Section 2.4.3, samples collected from the dissolution studies were analyzed using a validated HPLC method for St and a BCA kit for Sec. The analysis of the dissolution profiles over the 120-minute study demonstrated that both Sec and St completely transitioned into the dissolution medium at pH 5.6 (Fig. 2B). In a similar study, Yu et al. (Yu et al., 2021) developed HA-based dissolving microneedles loaded with doxorubicin, and the *in vitro* dissolution study demonstrated that approximately 95% of the active substance had transitioned into the dissolution medium by the end of the second hour.

The results of the *in vitro* dissolution experiment were evaluated using the KINETDS 3.0 application, revealing that the dissolution behaviors of both Sec and St followed Weibull release or dissolution kinetics. According to the Weibull model, drug release or dissolution primarily occurs through diffusion, followed by the disintegration of the polymer matrix. This aligns with the structural characteristics of microneedle drug delivery systems. Such dissolution behavior is particularly suitable for topical application (Xu et al., 2023).

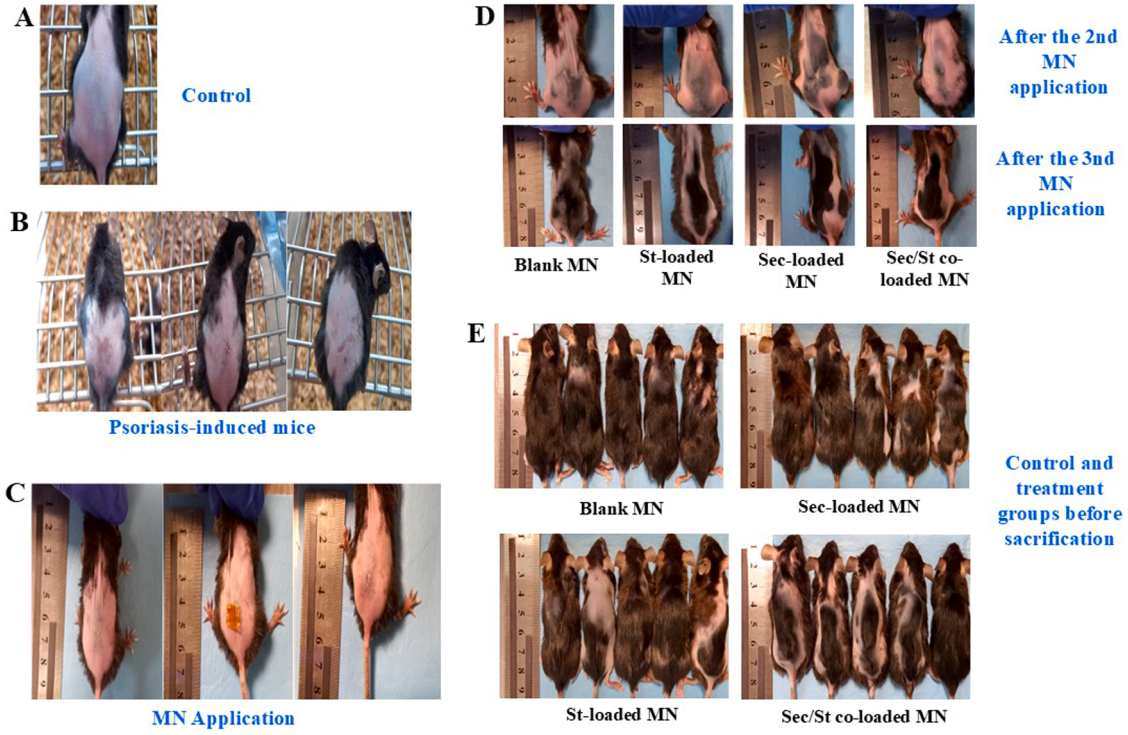


Fig. 8. Representative images of psoriasis model development and microneedle application in mice: **A.** Healthy mouse after one week of blank cream application (control); **B.** Psoriasis-induced mice after one week of imiquimod cream (5%) application; **C.** Representative image showing the application of the microneedle array onto the dorsal skin of the mouse; **D, E.** Images of the microneedle treatment process in mice.

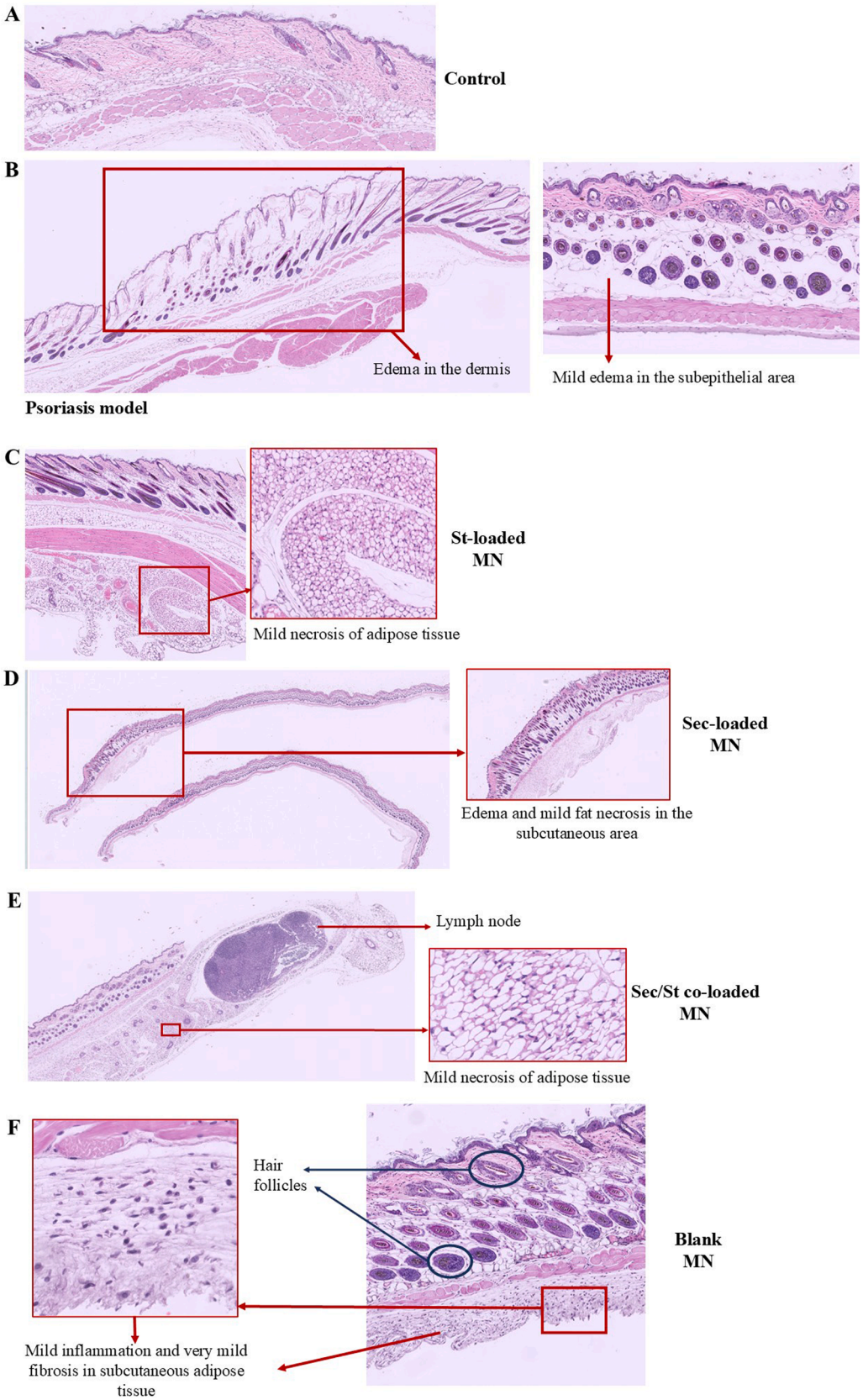


Fig. 9. Histological examination of mice skins; before (B) and after treatment (C-F). (A: Imiquimod-free cream applied control group, B: Indicators of psoriasis model development, C: Mild necrosis of adipose tissue observed following St-loaded MN application, D: Edema and mild fat necrosis in the subcutaneous area observed following Sec-loaded MN application, E: Mild necrosis of adipose tissue observed following Sec/St co-loaded MN application, F: Mild inflammation and very mild fibrosis in subcutaneous adipose tissue observed following blank MN application).

3.5. Safety evaluation of blank MNs

The time- and concentration-dependent cytotoxicity of MN matrix solution on L929 fibroblast cells was evaluated using the MTT assay. After 24 and 48 hours of incubation, cell viability remained above 75%, with values of 87.03% and 92.43% observed at the highest concentration (200 μg/mL), respectively (Fig. 7). Notably, cell viability exceeded 80% at all time points and concentrations, indicating that the hyaluronic acid and sucrose used in microneedle preparation do not exhibit cytotoxic effects on healthy cells (Srikanth et al., 2020). These results are consistent with the established biocompatibility of hyaluronic acid, which is commonly used in anti-aging fillers and various biomedical applications (Diepenbrock et al., 2017). Therefore, the polymer matrix was determined to be non-toxic to healthy fibroblast cells at tested concentrations (3.125-200 μg/mL), further supporting its safety profile for biomedical applications.

Similarly, in a study conducted by Cannella et al. (Cannella et al., 2020) on the safety of hyaluronic acid, various HA-containing fillers were applied to L929 cells. Cell viability was assessed at 24, 48, and 72 hours using the MTS assay. It was demonstrated that hyaluronic acid promotes cell proliferation, as indicated by an increase in cell growth over time in certain experimental groups, further supporting our findings.

3.6. In vivo evaluation of MN and histologic assessment

The formation of psoriasis lesions was visually confirmed by regional erythema and crusting (Fig. 8B), as well as by behavioral signs of discomfort, such as itching and restlessness. Additionally, histological analysis of skin sections using conventional optical microscopy further verified the formation of lesions. In the positive control group, an imiquimod-free cream was applied (Fig. 8A), and visual examination confirmed the absence of any reaction to the cream components.

During the treatment stage, cream application was discontinued, and microneedles were administered to psoriatic skin every three days (Fig. 8C). Although the therapeutic effect was not clearly visible after the second application, a significant reduction in scaling was observed by the third application in the group treated with Sec-loaded MNs (Fig. 8D). Two days following the final treatment, the backs of the mice were photographed under anesthesia, after which euthanasia was conducted for further analysis. By the end of the protocol (Fig. 8E), visual assessment of treatment efficacy became impractical due to the elongation of dorsal hairs in the mice. Therefore, treatment outcomes were evaluated through histological analysis of skin sections.

In the psoriasis treatment protocol, the percentage of inflammation observed in tissues showed a significant decrease after treatment with drug-loaded MNs (Table 2 and Fig. 9). However, no difference was observed between the experimental groups of St-loaded and Sec/St-loaded MNs. In the group where Sec was applied alone within the microneedle (Sec-loaded MN), no inflammation was observed, and a reduction in necrotic areas was also noted. In contrast, when Stattic and secukinumab were combined (Sec/St-loaded MN), increases in both necrotic areas and inflammation were observed. Consequently, the use of secukinumab alone, which acts as an inhibitor of inflammation-related cytokines, could be considered a long-term treatment option for psoriasis.

Although *in vivo* studies typically use a sample size of n=6 for statistical robustness, the statistical evaluation of our data with n=5 is supported by previous literature (Sathe et al., 2019; Stehlikova et al., 2019), demonstrating that reliable conclusions can be drawn with this sample size in similar experimental settings.

One limitation of this study is that it does not fully replicate the hallmark histological features of psoriasis in the animal model. Although some inflammatory and behavioral signs were evident, the absence of epidermal hyperplasia, parakeratosis, and Munro's abscesses limits the translational relevance of the observed therapeutic effects.

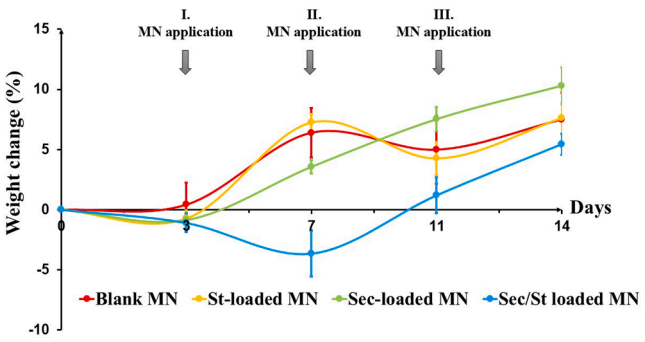


Fig. 10. Weight change of mice during the 14-day study period (n=5). MN applications were performed on days 3 (I), 7 (II), and 11 (III). Values are expressed as mean ± SD. Table 1 provides a detailed explanation of the formulation codes.

Body weights were recorded at baseline (day 0) and throughout the treatment period (up to day 14). No significant weight changes indicating adverse health effects were observed, and all groups exhibited weight gain over time (Fig. 10). Additionally, no survival-related concerns were noted, and all mice remained alive until the end of the experiment.

Overall, the visual and histological findings were consistent, suggesting that the therapeutic efficacy of psoriasis treatment could be improved by incorporating secukinumab into microneedles. While this study focused solely on evaluating the efficacy of the novel microneedle formulations, further research, including comparisons with standardized treatments, would provide more insight into their potential therapeutic use.

3.7. Immunologic examination

The effectiveness of MN formulations (as matrix solutions) to inhibit inflammatory pathways involved in the immunopathology of psoriasis was assessed using ELISA and Western blot analyses in *ex vivo* splenocyte cultures. It is well-established that fibroblasts produce elevated levels of IL-6, IL-8, and G-CSF cytokines under the influence of IL-17 (Yoyen-Ermis et al., 2019). Accordingly, a reduction in IL-6 levels was expected in groups treated with Sec. Notably, all microneedle-treated groups exhibited a significant decrease in IL-6 levels compared to those receiving drug solutions (Fig. 11A). This finding suggests that the microneedle matrix, composed of HA and sucrose, may play a role in modulating the immune response independently of the active pharmaceutical ingredient. HA, in particular, is known to suppress the production of inflammatory cytokines such as IL-6 and IL-8 and mediators (Hashizume and Mihara, 2010; Marinho et al., 2021; Rooney et al., 2015). Given that the inhibitory effect of HA on IL-6 production was found to be more pronounced than that of Sec, it is likely that this contributes to the consistent IL-6 inhibition observed across all microneedle-treated groups.

The *ex vivo* inhibition of the STAT3 pathway was evaluated using Western blot analysis. In this study, both phosphorylated (pSTAT3) and total STAT3 (tSTAT3) levels were found to be lower in the St-loaded MN groups compared to the St-solution group (Fig. 11B). These findings are consistent with previous reports indicating STAT3 inhibition by St under both *in vitro* (Arslan et al., 2023; Pan et al., 2013; Schust et al., 2006) and *ex vivo* (Guo et al., 2022) conditions. Similarly, STAT3 inhibition was also observed in microneedles containing only Sec. This effect is believed to result from a decrease in IL-6 production following IL-17A suppression, which may indirectly attenuate the JAK/STAT3 pathway (Wang et al., 2024).

It is important to note that splenocytes collected from mice in each group were pooled and analyzed in a single Western blot experiment due to limited sample availability. This approach restricts the quantitative

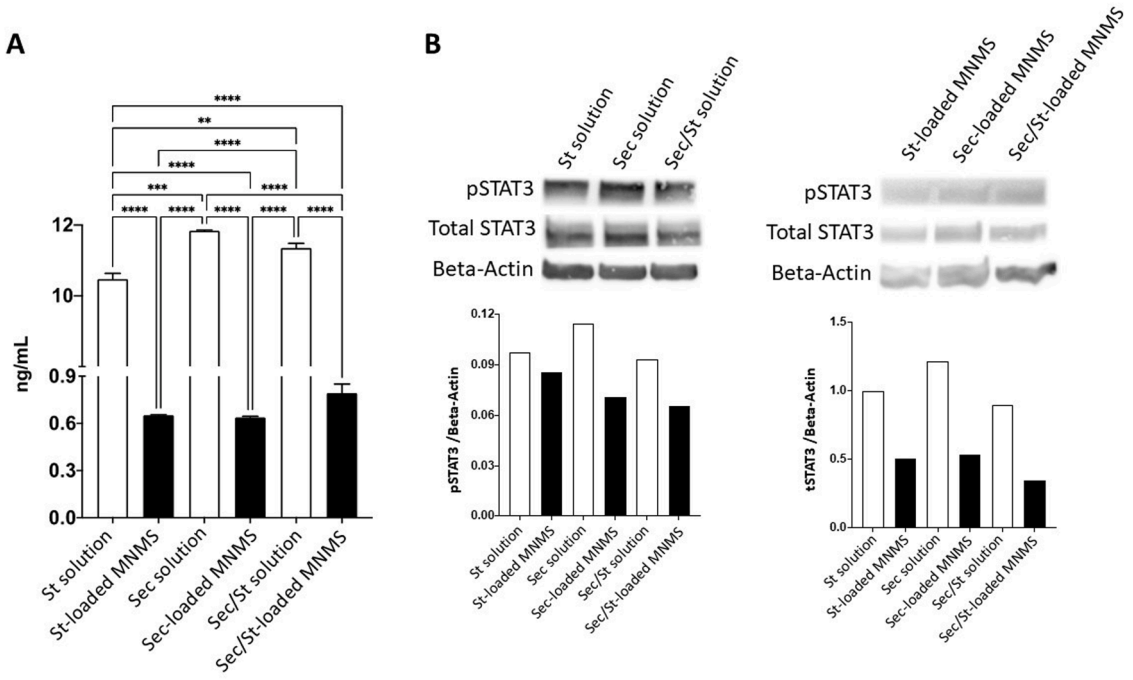


Fig. 11. Comparison of IL-6 gene expression (A) and STAT3 activation (B) in mouse splenocytes following application with drug solutions and microneedle matrix solutions via ELISA and Western Blot. ***p < 0.01, ***p < 0.001, ****p < 0.0001;* Ordinary one-way ANOVA test, each comparison stands alone (A).

interpretation of the protein expression data and represents a limitation of the current study.

According to the Western blot results, the group exhibiting the strongest STAT3 inhibition supports our hypothesis. Additionally, another notable finding is that loading the drugs into MNs enhanced STAT3 inhibition across all experimental conditions. As observed in the ELISA experiment, this outcome may be attributed to the composition of the microneedle formulation.

4. Conclusion

In this study, novel dissolving microneedle formulations encapsulating both secukinumab and Stattic were developed to enhance therapeutic efficacy in treating psoriasis. The combination aimed to inhibit both IL-17A-mediated immune activation and STAT3 signaling, which are both involved in the pathogenesis of the disease. Biocompatible polymers, such as hyaluronic acid and sucrose, were used as microneedle matrices to ensure safety, minimize toxicity, and support effective drug delivery.

An important aspect of this study is the use of microneedles for the treatment of psoriasis, which provides a safer, more effective, and patient-friendly method for drug delivery. Compared to intravenous administration of nanosystems, microneedle-based topical application offers a minimally invasive and painless alternative that promotes patient adherence. Overall, the findings indicate that while the combination of Stattic and secukinumab failed to enhance therapeutic efficacy, the microneedle-based delivery of secukinumab alone significantly improved treatment outcomes. These results highlight secukinumab-loaded microneedles as a promising and patient-friendly therapeutic approach for psoriasis, providing targeted efficacy with reduced systemic side effects. For further studies, it would be valuable to compare the efficacy of secukinumab-loaded microneedle formulation against conventional and standardized treatments for psoriasis. Additionally, it is important to investigate the long-term effects and safety profile of this delivery system.

CRediT authorship contribution statement

Meryem Kaplan: Writing – original draft, Visualization, Validation, Investigation, Data curation, Conceptualization. **Fatma Betül Arslan:** Writing – original draft, Visualization, Validation, Investigation, Data curation, Conceptualization. **Süleyman Can Öztürk:** Writing – review & editing, Data curation. **Sıla Ulutürk:** Writing – review & editing, Data curation. **Çisel Aydın Meriçöz:** Writing – review & editing, Data curation. **Güneş Esendağlı:** Writing – review & editing, Supervision, Conceptualization. **Sema Çalış:** Writing – review & editing, Supervision, Conceptualization. **Kivilcim Ozturk:** Writing – review & editing, Supervision, Project administration, Conceptualization.

Declaration of competing interest

The authors declare the following financial interests/personal relationships which may be considered as potential competing interests: Kıvılcım Öztürk reports the financial support was provided by Hacettepe University Scientific Research Project Foundation (Project No: TSA-2021-19005).

Data availability

Data will be made available on request.

References

Alexander, H., Nestle, F.O., 2017. Pathogenesis and immunotherapy in cutaneous psoriasis: what can rheumatologists learn? Curr. Opin. Rheumatol. 29 (1), 71–78. https://doi.org/10.1097/BOR.0000000000000358.

Alrimawi, B.H., Lee, J.Y., Ng, K.W., Goh, C.F., 2024. In vitro evaluation of microneedle strength: a comparison of test configurations and experimental insights. RSC Pharm 1 (2), 227–233. https://doi.org/10.1039/D4PM00024B.

Alunno, A., Bistoni, O., Bartoloni, E., Caterbi, S., Bigerna, B., Tabarrini, A., Mannucci, R., Falini, B., Gerli, R., 2013. IL-17-producing CD4− CD8− T cells are expanded in the peripheral blood, infiltrate salivary glands and are resistant to corticosteroids in patients with primary Sjögren's syndrome. Ann. Rheum. Dis. 72 (2), 286–292. https://doi.org/10.1136/annrheumdis-2012-201511.

Arslan, F.B., Öztürk, K., Tavukçuoğlu, E., Öztürk, S.C., Esendağlı, G., Çalış, S., 2023. A novel combination for the treatment of small cell lung cancer: Active targeted

irinotecan and stattic co-loaded PLGA nanoparticles. Int. J. Pharm. 632, 122573. https://doi.org/10.1016/j.ijpharm.2022.122573.
Berg, S.H., Balogh, E.A., Ghamrawi, R.I., Feldman, S.R., 2021. A review of secukinumab in psoriasis treatment. Immunotherapy. 13 (3), 201–216. https://doi.org/10.2217/imt-2020-0195.
Bodemer, A.A., 2023. Psoriasis. In: Rakel, D., Minichiello, V.J. (Eds.), Integrative Medicine. Elsevier, Amsterdam, pp. 620–630 fifth ed.
Cannella, V., Altomare, R., Leonardi, V., Russotto, L., Di Bella, S., Mira, F., Guercio, A., 2020. In vitro biocompatibility evaluation of nine dermal fillers on L929 cell line. Biomed. Res. Int. 2020 (1), 8676343. https://doi.org/10.1155/2020/8676343.
Chen, C.-H., Shyu, V.B.-H., Chen, C.-T., 2018. Dissolving microneedle patches for transdermal insulin delivery in diabetic mice: potential for clinical applications. Materials 11 (9), 1625. https://doi.org/10.3390/ma11091625.
Chi, Y., Huang, Y., Kang, Y., Dai, G., Liu, Z., Xu, K., Zhong, W., 2022. The effects of molecular weight of hyaluronic acid on transdermal delivery efficiencies of dissolving microneedles. Eur. J. Pharm. Sci. 168, 106075. https://doi.org/10.1016/j.ejps.2021.106075.
Coulman, S.A., Anstey, A., Gateley, C., Morrissey, A., McLoughlin, P., Allender, C., Birchall, J.C., 2009. Microneedle mediated delivery of nanoparticles into human skin. Int. J. Pharm. 366 (1-2), 190–200. https://doi.org/10.1016/j.ijpharm.2008.08.040.
Das, K., Ranjan, R., Kumar, P., Chandra, S., 2024. A comparative study of the effectiveness and safety of topical calcipotriol and topical methotrexate in chronic plaque psoriasis. Cureus. 16 (5), e59878. https://doi.org/10.7759/cureus.59878.
Dawud, H., Abu Ammar, A., 2023. Rapidly dissolving microneedles for the delivery of steroid-loaded nanoparticles intended for the treatment of inflammatory skin diseases. Pharmaceutics. 15 (2), 526. https://doi.org/10.3390/pharmaceutics15020526.
Soares de Sousa, A.M., Duarte, A.C., Decnop, M., de Faria Guimarães, D., Ferreira Coelho Neto, C.A., de Oliveira Sarpi, M., Palhiari Duarte, L.G., Ale Souza, S., Freire Segato, L., Diva Zavariz, J., Mukherji, S.K., 2023. Imaging features and complications of facial cosmetic procedures. Radiographics. 43 (12), e230060. https://doi.org/10.1148/rg.230060.
Diepenbrock, R.M., May, J.R., Cone Jr, W.R., Ehland, E.L., 2017. Patient preference for preprocedural anesthetic prior to facial cosmetic injectable fillers. Am. J. Cosmet. Surg. 34 (3), 143–149. https://doi.org/10.1177/0748806817690986.
Du, G., Sun, X., 2020. Current advances in sustained release microneedles. Pharmaceut. Fronts. 2, e11–e22. https://doi.org/10.1055/s-0040-1701435.
Du, H., Yang, J., Li, M., Xia, Y., Li, Y., Zhu, J., Zhang, L., Tao, J., 2024. Microneedle-assisted percutaneous delivery of methotrexate-loaded nanoparticles enabling sustained anti-inflammatory effects in psoriasis therapy. J. Mater. Chem. B 12 (10), 2618–2627. https://doi.org/10.1039/d3tb02643d.
Dubey, S., Sharma, R., Mody, N., Vyas, S.P., 2017. Novel carriers and approaches: insight for psoriasis management. In: Ficai, D., Grumezescu, A.M. (Eds.), Nanostructures for novel therapy. Elsevier, Amsterdam, pp. 657–684. https://doi.org/10.1016/B978-0-323-46142-9.00024-4.
Fletcher, S., Turkson, J., Gunning, P.T., 2008. Molecular approaches towards the inhibition of the signal transducer and activator of transcription 3 (Stat3) protein. ChemMedChem. 3 (8), 1159. https://doi.org/10.1002/cmdc.200800123.
Ghaferi, M., Alavi, S.E., Phan, K., Maibach, H., Mohammed, Y., 2024. Transdermal Drug Delivery Systems (TDDS): recent advances and failure modes. Mol. Pharm. 21, 5373–5391. https://doi.org/10.1021/acs.molpharmaceut.4c00211.
Gharibi, T., Babaloo, Z., Hosseini, A., Abdollahpour-Alitappeh, M., Hashemi, V., Marofi, F., Nejati, K., Baradaran, B., 2020. Targeting STAT3 in cancer and autoimmune diseases. Eur. J. Pharmacol. 878, 173107. https://doi.org/10.1016/j.ejphar.2020.173107.
Gomes, K.B., D'Souza, B., Vijayanand, S., Menon, I., D'Souza, M.J., 2022. A dual-delivery platform for vaccination using antigen-loaded nanoparticles in dissolving microneedles. Int. J. Pharm. 613, 121393. https://doi.org/10.1016/j.ijpharm.2021.121393.
Govindarajan, S., Elewaut, D., Drennan, M., 2015. An optimized method for isolating and expanding invariant natural killer T cells from mouse spleen. J. Vis. Exp. 104, 53256. https://doi.org/10.3791/53256.
Guillot, A.J., Cordeiro, A.S., Donnelly, R.F., Montesinos, M.C., Garrigues, T.M., Melero, A., 2020. Microneedle-based delivery: An overview of current applications and trends. Pharmaceutics. 12 (6), 569. https://doi.org/10.3390/pharmaceutics12060569.
Guo, H., Xiao, Y., Yuan, Z., Yang, X., Chen, J., Chen, C., Wang, M., Xie, L., Chen, Q., Tong, Y., Zhang, Q., Bai, Y., 2022. Inhibition of STAT3Y705 phosphorylation by Stattic suppresses proliferation and induces mitochondrial-dependent apoptosis in pancreatic cancer cells. Cell Death. Discov. 8 (1), 116. https://doi.org/10.1038/s41420-022-00922-9.
Hashizume, M., Mihara, M., 2010. High molecular weight hyaluronic acid inhibits IL-6-induced MMP production from human chondrocytes by up-regulating the ERK inhibitor, MKP-1. Biochem. Biophys. Res. Commun. 403 (2), 184–189. https://doi.org/10.1016/j.bbrc.2010.10.135.
Hawkes, J.E., Yan, B.Y., Chan, T.C., Krueger, J.G., 2018. Discovery of the IL-23/IL-17 signaling pathway and the treatment of psoriasis. J. Immun. 201 (6), 1605–1613. https://doi.org/10.4049/jimmunol.1800013.
He, X., Sun, J., Zhuang, J., Xu, H., Liu, Y., Wu, D., 2019. Microneedle system for transdermal drug and vaccine delivery: devices, safety, and prospects. Dose-Response 17 (4), 1559325819878585. https://doi.org/10.1177/1559325819878585.
Horváth, S., Komlódi, R., Perkecz, A., Pintér, E., Gyulai, R., Kemény, Á., 2019. Methodological refinement of Aldara-induced psoriasiform dermatitis model in mice. Sci. Rep. 9 (1), 3685. https://doi.org/10.1038/s41598-019-39903-x.
Huang, L., Luo, Y., Kuai, L., Zhang, X., Zhang, Y., Yang, Z., Fei, X., Sun, J., Luo, Y., Zhao, Y., Xue, T., Yin, W., Chang, J., Song, J., Li, Y., Li, B., Li, Y., 2025. An approach for psoriasis of microneedle patch simultaneously targeting multiple inflammatory cytokines and relapse related T cells. Biomater 318, 123120. https://doi.org/10.1016/j.biomaterials.2025.123120.
Huangfu, L., Li, R., Huang, Y., Wang, S., 2023. The IL-17 family in diseases: from bench to bedside. Sig. Transduct. Target. Ther. 8 (1), 402. https://doi.org/10.1038/s41392-023-01620-3.
Ighani, A., Partridge, A.C., Shear, N.H., Lynde, C., Gulliver, W.P., Sibbald, C., Fleming, P., 2019. Comparison of management guidelines for moderate-to-severe plaque psoriasis: a review of phototherapy, systemic therapies, and biologic agents. J. Cutan. Med. Surg. 23 (2), 204–221. https://doi.org/10.1177/1203475418814234.
Jang, M., Baek, S., Kang, G., Yang, H., Kim, S., Jung, H., 2020. Dissolving microneedle with high molecular weight hyaluronic acid to improve skin wrinkles, dermal density and elasticity. Int. J. Cosmet. Sci. 42 (3), 302–309. https://doi.org/10.1111/ics.12617.
Jha, A., Kumar, M., Goswami, P., Manjit, M., Bharti, K., Koch, B., Mishra, B., 2024. Hyaluronic acid-oleylamine and chitosan-oleic acid conjugate-based hybrid nanoparticle delivery via. dissolving microneedles for enhanced treatment efficacy in localized breast cancer. Biomater. Adv. 160, 213865. https://doi.org/10.1016/j.bioadv.2024.213865.
Jiang, X., Lillehoj, P.B., 2020. Microneedle-based skin patch for blood-free rapid diagnostic testing. Microsyst. Nanoeng. 6 (1), 96. https://doi.org/10.1038/s41378-020-00206-1.
Jung, J.H., Jin, S.G., 2021. Microneedle for transdermal drug delivery: current trends and fabrication. J. Pharm. Investig. 51 (5), 503–517. https://doi.org/10.1007/s40005-021-00512-4.
Kang, H., Zuo, Z., Lin, R., Yao, M., Han, Y., Han, J., 2022. The most promising microneedle device: present and future of hyaluronic acid microneedle patch. Drug Deliv. 29 (1), 3087–3110. https://doi.org/10.1080/10717544.2022.2125600.
Kim, D.-S., Choi, J.-T., Kim, C.B., Shin, Y.-R., Park, P.-G., Kim, H., Lee, J.M., Park, J.-H., 2020. Microneedle array patch (MAP) consisting of crosslinked hyaluronic acid nanoparticles for processability and sustained release. Pharm. Res. 37 (3), 50. https://doi.org/10.1007/s11095-020-2768-3.
Kochhar, J. S., Tan, J. J., Kwang, Y. C., Kang, L., 2019. Microneedles for transdermal drug delivery, first ed. Springer Cham, Switzerland AG. https://doi.org/10.1007/978-3-030-15444-8.
Larrañeta, E., Stewart, S., Fallows, S.J., Birkhäuer, L.L., McCrudden, M.T., Woolfson, A. D., Donnelly, R.F., 2016. A facile system to evaluate in vitro drug release from dissolving microneedle arrays. Int. J. Pharm. 497 (1-2), 62–69. https://doi.org/10.1016/j.ijpharm.2015.11.038.
Lé, A.M., Torres, T., 2022. New topical therapies for psoriasis. Am. J. Clin. Dermatol. 23 (1), 13–24. https://doi.org/10.1007/s40257-021-00649-w.
Lee, H.-J., Kim, M., 2023. Challenges and future trends in the treatment of psoriasis. Int. J. Mol. Sci. 24 (17), 13313. https://doi.org/10.3390/ijms241713313.
Lee, J.W., Park, J.-H., Prausnitz, M.R., 2008. Dissolving microneedles for transdermal drug delivery. Biomater 29 (13), 2113–2124. https://doi.org/10.1016/j.biomaterials.2007.12.048.
Li, J., Yuan, Z., Shi, S., Chen, X., Yu, S., Qi, X., Deng, T., Zhou, Y., Tang, D., Xu, S., Zhang, J., Jiao, Y., Yu, W., Wang, L., Yang, L., Gao, P., 2024. Microneedle patches incorporating zinc-doped mesoporous silica nanoparticles loaded with betamethasone dipropionate for psoriasis treatment. J. Nanobiotechnology. 22 (1), 706. https://doi.org/10.1186/s12951-024-02986-4.
Marinho, A., Nunes, C., Reis, S., 2021. Hyaluronic acid: a key ingredient in the therapy of inflammation. Biomolecules. 11 (10), 1518. https://doi.org/10.3390/biom11101518.
McGeachy, M.J., Cua, D.J., Gaffen, S.L., 2019. The IL-17 family of cytokines in health and disease. Immunity. 50 (4), 892–906. https://doi.org/10.1016/j.immuni.2019.03.021.
Miao, M., Yan, J., Sun, Y., Liu, J., Guo, S., 2025. Psoriasis: unraveling disease mechanisms and advancing pharmacological and nanotechnological treatments. J. Inflamm. Res. 18, 2045–2072. https://doi.org/10.2147/JIR.S506103.
Nagarkar, R., Singh, M., Nguyen, H.X., Jonnalagadda, S., 2020. A review of recent advances in microneedle technology for transdermal drug delivery. J. Drug Deliv. Sci. Technol. 59, 101923. https://doi.org/10.1016/j.jddst.2020.101923.
Nakae, S., Saijo, S., Horai, R., Sudo, K., Mori, S., Iwakura, Y., 2003. IL-17 production from activated T cells is required for the spontaneous development of destructive arthritis in mice deficient in IL-1 receptor antagonist. Proc. Natl. Acad. Sci. U.S.A. 100 (10), 5986–5990. https://doi.org/10.1073/pnas.1035999100.
Pan, Y., Zhou, F., Zhang, R., Claret, F.X., 2013. Stat3 inhibitor Stattic exhibits potent antitumor activity and induces chemo-and radio-sensitivity in nasopharyngeal carcinoma. PLoS. One 8 (1), e54565. https://doi.org/10.1371/journal.pone.0054565.
Papp, K.A., Lebwohl, M., 2018. Onset of Action of Biologics in Patients With Moderate-to-Severe Psoriasis. J. Drugs Dermatol. 17 (3), 247–250. PMID: 29537442.
Phillips, D.J., Pygall, S.R., Cooper, V.B., Mann, J.C., 2012. Overcoming sink limitations in dissolution testing: a review of traditional methods and the potential utility of biphasic systems. J. Pharm. Pharmacol. 64 (11), 1549–1559. https://doi.org/10.1111/j.2042-7158.2012.01523.x.
Pradhan, M., Alexander, A., Singh, M.R., Singh, D., Saraf, S., Saraf, S., 2018. Understanding the prospective of nano-formulations towards the treatment of psoriasis. Biomed. PharmacOther 107, 447–463. https://doi.org/10.1016/j.biopha.2018.07.156.
Raharja, A., Mahil, S.K., Barker, J.N., 2021. Psoriasis: a brief overview. Clin. Med. 21 (3), 170–173. https://doi.org/10.7861/clinmed.2021-0257.

Ramic, L., Sator, P., 2023. Topical treatment of psoriasis vulgaris. J. Dtsch. Dermatol. Ges. 21 (6), 631–642. https://doi.org/10.1111/ddg.15042.
Rehman, N.U., Song, C., Kim, J., Noh, I., Rhee, Y.-S., Chung, H.J., 2021. Pharmacokinetic Evaluation of a Novel Donepezil-Loaded Dissolving Microneedle Patch in Rats. Pharmaceutics. 14 (1), 5. https://doi.org/10.3390/pharmaceutics14010005.
Reichrath, J., Holick, M.F., 2018. Psoriasis and other skin diseases. In: Feldman, David (Ed.), Vitamin D. Elsevier, Amsterdam, pp. 1037–1051. https://doi.org/10.1016/b978-0-12-381978-9.10097-6.
Rooney, P., Srivastava, A., Watson, L., Quinlan, L.R., Pandit, A., 2015. Hyaluronic acid decreases IL-6 and IL-8 secretion and permeability in an inflammatory model of interstitial cystitis. Acta Biomater. 19, 66–75. https://doi.org/10.1016/j.actbio.2015.02.030.
Sakai, K., Sanders, K.M., Youssef, M.R., Yanushefski, K.M., Jensen, L., Yosipovitch, G., Akiyama, T., 2016. Mouse model of imiquimod-induced psoriatic itch. Pain. 157 (11), 2536. https://doi.org/10.1097/j.pain.0000000000000674.
Salih, A.R.C., Farooqi, H.M.U., Amin, H., Karn, P.R., Meghani, N., Nagendran, S., 2024. Hyaluronic acid: Comprehensive review of a multifunctional biopolymer. Futur. J. Pharm. Sci. 10 (1), 63. https://doi.org/10.1186/s43094-024-00636-y.
Sartawi, Z., Blackshields, C., Faisal, W., 2022. Dissolving microneedles: applications and growing therapeutic potential. J. Contr. Release. 348, 186–205. https://doi.org/10.1016/j.jconrel.2022.05.045.
Sathe, P., Saka, R., Kommineni, N., Raza, K., Khan, W., 2019. Dithranol-loaded nanostructured lipid carrier-based gel ameliorate psoriasis in imiquimod-induced mice psoriatic plaque model. Drug Dev. Ind. Pharm. 45 (5), 826–838. https://doi.org/10.1080/03639045.2019.1576722.
Schust, J., Sperl, B., Hollis, A., Mayer, T.U., Berg, T., 2006. Stattic: a small-molecule inhibitor of STAT3 activation and dimerization. Chem. Biol. 13 (11), 1235–1242. https://doi.org/10.1016/j.chembiol.2006.09.018.
Shin, J.Y., Han, D., Yoon, K.Y., Jeong, D.H., Park, Y.I., 2024. Clinical safety and efficacy evaluation of a dissolving microneedle patch having dual anti-wrinkle effects with safe and long-term activities. Ann. Dermatol. 36 (4), 215. https://doi.org/10.5021/ad.23.136.
Srikanth, M., Khan, W.S., Asmatulu, R., Misak, H.E., Yang, S.-Y., Asmatulu, E., 2020. In vitro cytotoxicity studies of industrially used common nanomaterials on L929 and 3T3 fibroblast cells. J. Biomed. Res. Environ. Sci. 1 (5), 192–200. https://doi.org/10.37871/jbres1143.
Stehlikova, Z., Kostovcikova, K., Kverka, M., Rossmann, P., Dvorak, J., Novosadova, I., Kostovcik, M., Coufal, S., Srutkova, D., Prochazkova, P., 2019. Crucial role of microbiota in experimental psoriasis revealed by a gnotobiotic mouse model. Front. Microbiol. 10, 236. https://doi.org/10.3389/fmicb.2019.00236.
Sun, X., Cui, Z., Wang, Q., Liu, L., Ding, X., Wang, J., Cai, X., Li, B., Li, X., 2024. Formation and clinical effects of anti-drug antibodies against biologics in psoriasis treatment: an analysis of current evidence. Autoimmun. Rev. 23 (4), 103530. https://doi.org/10.1016/j.autrev.2024.103530.
Ti, C., Chen, H., Zhou, W., Bian, A., Hu, P., Miao, Y., Shao, T., Liu, M., Chen, Y., Yi, Z., 2024. WB518, a novel STAT3 inhibitor, effectively alleviates IMQ and TPA-induced animal psoriasis by inhibiting STAT3 phosphorylation and Keratin 17. Int. Immunopharmacol. 127, 111344. https://doi.org/10.1016/j.intimp.2023.111344.
Valachová, K., Šoltés, L., 2021. Hyaluronan as a prominent biomolecule with numerous applications in medicine. Int. J. Mol. Sci. 22 (13), 7077. https://doi.org/10.3390/ijms22137077.
Wang, F., Li, Y., Yang, Z., Cao, W., Liu, Y., Zhao, L., Zhang, T., Zhao, C., Yu, J., Yu, J., Zhou, J., Zhang, X., Li, P.P., Han, M., Feng, S., Ng, B.W.L., H, Z.W., Jiang, E., Li, K., Cui, B., 2024. Targeting IL-17A enhances imatinib efficacy in Philadelphia chromosome-positive B-cell acute lymphoblastic leukemia. Nat. Commun. 15 (1), 203. https://doi.org/10.1038/s41467-023-44270-3.
Worm, M., Sterry, W., 2006. Non-bullous skin diseases: alopecia, vitiligo, psoriasis, and urticaria. In: Mackay, I.R., Rose, N.R. (Eds.), The Autoimmune Diseases. Elsevier /Academic Press, Amsterdam, pp. 811–814 fourth ed.
Xia, C., Fu, X., Wang, Q., Chen, X., Chen, J., Kang, Y., Wang, B., 2024. Anti-ROS and NIR-II-Responsive Hyaluronic Acid Microneedle Loaded With Baicalin Nanoparticles for Treatment of Psoriasis. Macromol. Rapid. Commun. 45 (15), 2400136. https://doi.org/10.1002/marc.202400136.
Xu, S., Liu, W., Peng, M., Ma, D., Liu, Z., Tang, L., Li, X., Chen, S., 2023. Biodegradable microneedles array with dual-release behavior and parameter optimization by finite element analysis. J. Pharm. Sci. 112 (9), 2506–2515. https://doi.org/10.1016/j.xphs.2023.04.007.
Yan, Q., Weng, J., Shen, S., Wang, Y., Fang, M., Zheng, G., Yang, Q., Yang, G., 2021. Finite element analysis for biodegradable dissolving microneedle materials on skin puncture and mechanical performance evaluation. Polymers. (Basel) 13 (18), 3043. https://doi.org/10.3390/polym13183043.
Yang, L., Li, B., Dang, E., Jin, L., Fan, X., Wang, G., 2016. Impaired function of regulatory T cells in patients with psoriasis is mediated by phosphorylation of STAT3. J. Dermatol. Sci. 81 (2), 85–92. https://doi.org/10.1016/j.jdermsci.2015.11.007.
Yoyen-Ermis, D., Tunali, G., Tavukcuoglu, E., Horzum, U., Ozkazanc, D., Sutlu, T., Buyukasik, Y., Esendagli, G., 2019. Myeloid maturation potentiates STAT3-mediated atypical IFN-γ signaling and upregulation of PD-1 ligands in AML and MDS. Sci. Rep. 9 (1), 11697. https://doi.org/10.1038/s41598-019-48256-4.
Yu, M., Lu, Z., Shi, Y., Du, Y., Chen, X., Kong, M., 2021. Systematic comparisons of dissolving and swelling hyaluronic acid microneedles in transdermal drug delivery. Int. J. Biol. Macromol. 191, 783–791. https://doi.org/10.1016/j.ijbiomac.2021.09.161.
Zeng, Y., Wu, L., Jiang, X., Hu, Y., Jin, Y., Hu, H., Li, W., 2025. Self-assembled hyaluronic acid nanoparticles delivered by polymeric microneedles for targeted and long-acting therapy of psoriasis. Int. J. Pharm. 669, 125073. https://doi.org/10.1016/j.ijpharm.2024.125073.
Zhang, P., Wu, M.X., 2018. A clinical review of phototherapy for psoriasis. Lasers. Med. Sci. 33 (1), 173–180. https://doi.org/10.1007/s10103-017-2360-1.
Zhao, Z., Chen, Y., Shi, Y., 2020. Microneedles: a potential strategy in transdermal delivery and application in the management of psoriasis. RSC. Adv. 10 (24), 14040–14049. https://doi.org/10.1039/d0ra00735h.